



**HAL**  
open science

## Investigating the neuroprotective effect of AAV-mediated $\beta$ -synuclein overexpression in a transgenic model of synucleinopathy

Dorian Sargent, Dominique Bétemps, Matthieu Drouyer, Jérémy Verchere,  
Damien Gaillard, Jean-Noël Arzac, Latifa Lakhdar, Thierry Baron, Anna  
Salvetti

### ► To cite this version:

Dorian Sargent, Dominique Bétemps, Matthieu Drouyer, Jérémy Verchere, Damien Gaillard, et al..  
Investigating the neuroprotective effect of AAV-mediated  $\beta$ -synuclein overexpression in a transgenic  
model of synucleinopathy. *Scientific Reports*, 2018, 8, pp.17563. 10.1038/s41598-018-35825-2 . hal-  
03326879

**HAL Id: hal-03326879**

**<https://hal.science/hal-03326879>**

Submitted on 26 Aug 2021

**HAL** is a multi-disciplinary open access archive for the deposit and dissemination of scientific research documents, whether they are published or not. The documents may come from teaching and research institutions in France or abroad, or from public or private research centers.

L'archive ouverte pluridisciplinaire **HAL**, est destinée au dépôt et à la diffusion de documents scientifiques de niveau recherche, publiés ou non, émanant des établissements d'enseignement et de recherche français ou étrangers, des laboratoires publics ou privés.

1

2 **Investigating the neuroprotective effect of AAV-mediated  $\beta$ -synuclein overexpression in**  
3 **a transgenic model of synucleinopathy**

4

5

6 Dorian Sargent<sup>1</sup>, Dominique Bétemps<sup>1</sup>, Matthieu Drouyer<sup>1</sup>, Jérémy Verchere<sup>1</sup>, Damien

7 Gaillard<sup>1</sup>, Jean-Noël Arzac<sup>1</sup>, Latifa Lakhdar<sup>1</sup>, Anna Salvetti<sup>2</sup>, Thierry Baron<sup>1\*</sup>

8

9 <sup>1</sup> ANSES (French Agency for Food, Environmental and Occupational Health & Safety),

10 University of Lyon, Lyon, France

11 <sup>2</sup> INSERM U1052, Cancer Research Center of Lyon (CRCL), CNRS UMR 5286,

12 University of Lyon, Lyon, France

13

14

15

16 \* Corresponding author: Thierry Baron, ANSES - Laboratoire de Lyon, 31, avenue Tony

17 Garnier 69364 Lyon cedex 7; [thierry.baron@anses.fr](mailto:thierry.baron@anses.fr); Tel: +33 (0)4 78 69 68 33; Fax: +33

18 (0)4 78 61 91 45

19

20 Abstract word count: 199

21 Main text word count: 4233

22

23

24 **ABSTRACT**

25 Parkinson's disease (PD) and multiple system atrophy (MSA) are neurodegenerative diseases  
26 characterized by inclusions mainly composed of  $\alpha$ -synuclein ( $\alpha$ -syn) aggregates. The  
27 objective of this study was to investigate if  $\beta$ -synuclein ( $\beta$ -syn) overexpression could have  
28 beneficial effects by inhibiting the aggregation of  $\alpha$ -syn. The M83 transgenic mouse is a  
29 model of synucleinopathy, which develops severe motor symptoms associated with  
30 aggregation of  $\alpha$ -syn. M83 neonate or adult mice were injected with adeno-associated virus  
31 vectors carrying the human  $\beta$ -syn gene (AAV $\beta$ -syn) or green fluorescent protein gene  
32 (AAVGFP) using different injection sites. The M83 disease was - or not - accelerated using  
33 extracts of M83 brains injected with brain extract from mouse (M83) or human (MSA)  
34 origins. AAV vectors expression was confirmed using Western blot and ELISA technics.  
35 AAV mediated  $\beta$ -syn overexpression did not delay the disease onset or reduce the  $\alpha$ -syn  
36 phosphorylated at serine 129 levels detected by ELISA, regardless of the AAV injection route  
37 and the inoculation of brain extracts. Instead, a proteinase-K resistant  $\beta$ -syn staining was  
38 detected by immunohistochemistry, specifically in sick M83 mice overexpressing  $\beta$ -syn after  
39 inoculation of AAV $\beta$ -syn. This study indicated for the first time that viral vector-mediated  $\beta$ -  
40 syn overexpression could form aggregates in a model of synucleinopathy.

41

42

## 43 **Introduction**

44            Parkinson's disease (PD), dementia with Lewy bodies (DLB) and multiple system  
45 atrophy (MSA) are synucleinopathies, characterized by inclusions mainly composed of an  
46 aggregated form of  $\alpha$ -synuclein ( $\alpha$ -syn) in the central nervous system (CNS). As for prions,  
47 aggregated forms of  $\alpha$ -syn propagate within the CNS during the associated neuro-  
48 degenerative diseases. This characteristic was initially suggested in humans by Braak's  
49 description of PD stages, and was confirmed later in experimental models of  
50 synucleinopathies, in particular in the M83 transgenic mouse model <sup>1</sup>. M83 mice express the  
51 human A53T mutated  $\alpha$ -syn found in some familial PD forms, under the control of the mouse  
52 prion promoter <sup>1</sup>. These mice spontaneously develop severe motor impairment at 8-16 months  
53 of age at the homozygous state. The symptomatology is associated with the accumulation in  
54 the CNS, of a pathological form of  $\alpha$ -syn ( $\alpha$ -syn<sup>P</sup>), heavily phosphorylated at serine 129  
55 residue. We previously showed that, in M83 mice, disease onset can be accelerated by the  
56 intracerebral inoculation of brain homogenates from sick M83 mice <sup>2</sup>. This model was further  
57 characterized by development of an original ELISA that specifically detects, and allows to  
58 easily quantify, the pathological  $\alpha$ -syn in sick M83 mice <sup>3-5</sup>. This *in vivo* model may be useful  
59 for testing novel therapeutic strategies, particularly targeting progression of the  $\alpha$ -syn  
60 aggregation.

61  $\beta$ -synuclein ( $\beta$ -syn) is another member of the synuclein family, lacking a part of the non-  
62 amyloid component, a specific region suggested to be amyloidogenic in  $\alpha$ -syn. According to  
63 *in vitro* studies, unlike  $\alpha$ -syn,  $\beta$ -syn alone is not able to form aggregates, but could instead  
64 interact with  $\alpha$ -syn and reduce its capacity to aggregate <sup>6</sup>. These anti-aggregative features  
65 have been investigated *in vivo*, and some of these studies indeed reported a neuroprotective  
66 effect and reduction of  $\alpha$ -syn inclusions after overexpression of the human  $\beta$ -syn mediated by  
67 DNA microinjection or lentiviral vectors in the transgenic D mouse model, overexpressing

68 human wild-type  $\alpha$ -syn<sup>7,8</sup>. Another study also suggested that crossing mice overexpressing  
69 human  $\beta$ -syn with M83 mice delayed the M83 disease onset and reduced the  $\alpha$ -syn  
70 aggregation<sup>9</sup>. However, two recent studies by Taschenberger *et al* and Landeck *et al* which  
71 analyzed the impact of human  $\beta$ -syn overexpression mediated by adeno-associated viral  
72 vectors (AAV) on nigral dopaminergic neurons in rats, described a neurodegeneration with  $\beta$ -  
73 syn aggregates<sup>10,11</sup>.

74 Here, in order to assess the effects of  $\beta$ -syn overexpression in the context of these recent and  
75 unexpected data suggesting that  $\beta$ -syn produced using AAV may be able to aggregate, we  
76 investigated the impact of human  $\beta$ -syn overexpression mediated by AAV on the onset of the  
77 synucleinopathy of M83 mice. Two strategies of inoculation of the AAV vector were  
78 sequentially tested: (i) an intracerebroventricular (ICV) inoculation at birth, in order to  
79 generate a widespread overexpression of the vector in the central nervous system<sup>12</sup>, and (ii)  
80 an inoculation of the AAV vector into the ventral tegmental area (VTA)<sup>13</sup>, a region of the  
81 mesencephalon in which prominent  $\alpha$ -syn aggregation occurs in sick M83 mice<sup>1</sup>. Our results  
82 indicate that, regardless of the AAV inoculation strategy, continuous AAV-mediated  $\beta$ -syn  
83 overexpression in neurons did not delay the onset of the disease and did not modify the  $\alpha$ -syn<sup>P</sup>  
84 levels measured by ELISA, strongly suggesting that  $\beta$ -syn may not protect against  $\alpha$ -syn  
85 aggregation and propagation.

86

## 87 **Results**

### 88 **Human $\beta$ -syn is widely expressed after intracerebroventricular injection of AAV $\beta$ -syn in** 89 **neonates**

90 To overexpress  $\beta$ -syn in the M83 CNS, we used self-complementary (sc)AAV9 vectors  
91 expressing human  $\beta$ -syn (AAV $\beta$ -syn) gene or, as a control, the green fluorescent protein

92 (AAVGFP) gene under the control of the human synapsin1 promoter and with a post-  
93 transcriptional WPRE regulatory sequence (Supplementary figure 1A).

94 To functionally evaluate the AAV vectors, we first inoculated AAV $\beta$ -syn in the right and left  
95 cerebral ventricles of wild-type B6C3H newborn mice (genetic background of M83 transgenic  
96 mice) to obtain a widespread expression of the transgene in the CNS<sup>12</sup>. One month later,  
97 using viral specific primers, vector mRNA was detected in all regions of the brain and in the  
98 spinal cord (Supplementary figure 1B), as described<sup>14</sup>, with higher levels in rostral regions of  
99 the brain (olfactory bulbs, cortex, hippocampus, striatum) and mesencephalon.

100

#### 101 **Intracerebroventricular injection of AAV $\beta$ -syn did not modify the disease of M83 mice**

102 AAV vectors were first tested in M83 mice challenged by inoculation of brain extracts from  
103 sick M83 mice, an experimental design which is characterized by a quicker onset of the  
104 disease with a lower intragroup variability as compared to unchallenged M83 mice<sup>2</sup>. AAV  
105 vectors were ICV inoculated at birth and two months later challenged with different brain  
106 extracts of sick M83 mice, one derived from a second passage of a sick M83 brain extract in  
107 M83 mice (M83/M83 inoculum), and the other from a second passage of a human brain  
108 extract from a MSA patient in M83 mice (MSA/M83 inoculum) (Figure 1A, Supplementary  
109 table 1)<sup>5</sup>. M83 mice were euthanized after the detection of the first symptoms of disease, *i.e*  
110 balance disorders or hind limb paralysis, identified by two independent observers.

111 In both experiments, no delay in the onset of the disease was observed in AAV $\beta$ -syn injected  
112 mice as compared to control AAVGFP mice, regardless of the type of inoculum (M83/M83 or  
113 MSA/M83). Instead, AAV $\beta$ -syn injection significantly accelerated the onset of the disease in  
114 animals challenged with the M83/M83 extract as compared to control mice (log rank test  
115  $p < 0,05$ ) (Figure 1B). In contrast, no difference was observed in animals challenged with the  
116 MSA/M83 extract (Figure 1E). In each experiment, we did not detect any difference

117 concerning the clinical symptoms of sick mice after the injection of AAV $\beta$ -syn or AAVGFP.  
118 After dissection of the brains, biochemical analyses were realized. As the vector expression  
119 was higher in the rostral regions of the brain than in other CNS regions after ICV injections,  
120 we first checked the vector expression by detecting total  $\beta$ -syn in the hippocampus. An  
121 ELISA test adapted from Krassnig *et al.* allowed to detect a significant overexpression of  $\beta$ -  
122 syn (both murine  $\beta$ -syn and human  $\beta$ -syn produced by the vector) in the hippocampus,  
123 confirming the continuous expression of the AAV $\beta$ -syn until the disease onset (Figure 1C,  
124 and F). We next focused on the mesencephalon, the brainstem and the spinal cord because  
125 these CNS regions are known to be strongly positive in  $\alpha$ -syn<sup>P</sup> in sick M83 mice <sup>3-5</sup>. A  
126 significant overexpression of  $\beta$ -syn was only detected in the mesencephalon, the brain stem  
127 and in the spinal cord of sick M83 mice injected with AAV $\beta$ -syn challenged with M83/M83  
128 inoculum, but not in mice challenged with the MSA/M83 inoculum (Figure 1C and F). Since  
129 the M83 disease is associated with moderate or high  $\alpha$ -syn<sup>P</sup> levels into different brain regions  
130 and in the spinal cord <sup>5</sup>, we quantified  $\alpha$ -syn<sup>P</sup> using ELISA in order to detect a potential effect  
131 of  $\beta$ -syn on this biochemical marker of the disease. Our analyses did not show any significant  
132 difference in the  $\alpha$ -syn<sup>P</sup> levels in any of the examined CNS regions after AAV $\beta$ -syn  
133 inoculation, regardless of the nature of the inoculum used to accelerate the disease (Figure  
134 1D, and G).

135 To further study the levels of  $\beta$ -syn protein after AAV injections in M83 mice throughout the  
136 CNS, we used Western blot and ELISA which allowed to detect total  $\beta$ -syn in specific brain  
137 regions. Comparing total  $\beta$ -syn levels of 5 to 7 months old sick M83 mice inoculated at birth  
138 with AAV $\beta$ -syn or AAV GFP then challenged with the MSA/M83 inoculum (same mice as in  
139 Figure 1E), an overexpression of  $\beta$ -syn protein was detected by ELISA in the olfactory bulbs,  
140 cortex, striatum, hippocampus, but not in the other regions (Figure 2A), consistent with the  
141 results obtained by qRT-PCR at one month after AAV inoculation (Supplementary figure 1B).

142 Western blot analyses confirmed an overexpression of  $\beta$ -syn protein in the hippocampus of  
143 the same mice after AAV $\beta$ -syn inoculation (Figure 2B and C). Most of the animals inoculated  
144 with AAV $\beta$ -syn showed a  $\beta$ -syn overexpression detectable until the disease onset (Figure 1C,  
145 F). Only a few animals did not show significant overexpression of  $\beta$ -syn detected by ELISA  
146 or by immunohistochemistry (5/48 animals, in the entire study); these animals were excluded  
147 for the study analyzing the onset of disease.

148 We next examined the possible effects of AAV $\beta$ -syn ICV injection on the spontaneous  
149 development of the M83 disease during aging, without any challenge to accelerate the disease  
150 (Figure 3A). Here again, AAV $\beta$ -syn injection neither delayed the disease onset of M83 mice  
151 nor modified the  $\alpha$ -syn<sup>P</sup> levels (Figure 3B and D), despite a sustained expression of the  
152 transgene, at least in the hippocampus, up to the disease onset (Figure 3C) (ELISA data  
153 correspond to 2 mice for the treated group and 3 mice for the control group; consequently, no  
154 statistical analysis was done here).

155 Altogether, these results indicated that AAV $\beta$ -syn injection in the ventricles resulted in a  
156 widespread expression of the transgene in the CNS, but at a moderate level, especially in the  
157 structures that are the most heavily affected by the synucleinopathy lesions. We thus  
158 considered another strategy by inoculating the AAV vectors in the ventral tegmental area  
159 (VTA), which is located into the mesencephalon, where major brain lesions and accumulation  
160 of  $\alpha$ -syn<sup>P</sup> are detected in sick M83 mice and which is also connected to multiple brain areas  
161 <sup>13</sup>.

162

### 163 **$\beta$ -syn is overexpressed mostly in the mesencephalon after injection of AAV $\beta$ -syn in the** 164 **VTA of adult mice**

165 In order to validate this injection protocol of AAV vectors into the VTA, two months old  
166 wild-type mice were first inoculated with AAV $\beta$ -syn in the VTA and sacrificed one month

167 later. After dissection of the brains, vector mRNA was mostly detected in the mesencephalon,  
168 but also in the cortex, striatum, hippocampus and brainstem; only traces of vector mRNA  
169 were identified in the other regions of the brain (except the olfactory bulbs) and in the spinal  
170 cord, as compared to mesencephalon (Supplementary figure 1C).

171

### 172 **Injection of AAV $\beta$ -syn in the VTA did not modify the disease of M83 mice**

173 The same protocol was then applied to M83 mice. After the inoculation of AAV in the VTA  
174 in two months old M83 mice, the disease was accelerated by intracerebrally inoculating the  
175 mice one month later with the M83/M83 or the MSA/M83 inoculum (Figure 4A). No  
176 significant difference in the survival was observed between the AAV $\beta$ -syn and AAVGFP  
177 injected mice, between 3 and 8 months (Figure 4B, E). As before, we did not detect any  
178 difference concerning the clinical symptoms of sick mice after the injection of AAV $\beta$ -syn or  
179 AAVGFP. Importantly, analyses by ELISA confirmed the strong overexpression of  $\beta$ -syn in  
180 the mesencephalon although no difference was detected in the levels of pathological  $\alpha$ -syn<sup>P</sup> at  
181 the disease stage (Figure 4C, D, F, and G).

182 By immunohistochemistry, using an antibody targeting total  $\beta$ -syn (human and murine  $\beta$ -syn),  
183 a specific  $\beta$ -syn staining punctate pattern was detected in the inoculated mesencephalon, as  
184 well as in the striatum and brain stem which represent connected regions<sup>13</sup>, of all the sick  
185 M83 mice inoculated with AAV $\beta$ -syn (5/5), but not in sick M83 mice inoculated with  
186 AAVGFP (0/2) (Figure 4H). Further analysis indicated that these  $\beta$ -syn immunoreactive dots,  
187 which are specifically detected in mice inoculated with AAV $\beta$ -syn, mostly co-localize with  
188 the presynaptic protein synaptophysin (Supplementary figure 2A). Co-localization of GFP  
189 with neuronal marker  $\beta$ -tubulin type 3 in sick M83 mice inoculated with AAVGFP also  
190 confirmed that these vectors allowed a neuronal specific expression of the transgene  
191 (Supplementary figure 2B). Interestingly, the morphology of the inclusions containing  $\alpha$ -syn

192 phosphorylated at serine 129 detected by immunohistochemistry was not modified by  $\beta$ -syn  
193 overexpression (Supplementary figure 3A). Furthermore, these inclusions only rarely co-  
194 localized with AAV-specific  $\beta$ -syn staining by immunofluorescence (Supplementary figure  
195 3B). We further biochemically characterized vectors expression after injection in the VTA in  
196 M83 mice euthanized 4 months later. Total  $\beta$ -syn levels were quantified by ELISA and  
197 showed a significant increase of the protein in the mesencephalon of mice injected with  
198 AAV $\beta$ -syn as well as in the hippocampus and brain stem compared to control mice injected  
199 with the AAVGFP (Figure 5A).  $\beta$ -syn protein overexpression was also readily detected by  
200 Western blot in the mesencephalon of most of these mice (Figure 5B).

201

### 202 **The absence of protective effect was not due to an insufficient dose of AAV vector** 203 **injected in the VTA**

204 We finally asked whether the absence of any significant effect of AAV $\beta$ -syn could be due to  
205 an insufficient dose of AAV vector. We thus injected 4-times more vector in the VTA one  
206 month before the challenge by intra-cerebral inoculation of the M83/M83 inoculum. This  
207 AAV dose allowed to significantly increase the overexpression of  $\beta$ -syn at the disease stage  
208 ( $p < 0,05$ ) (Figure 5C, D). However, the M83 disease was still not delayed by  $\beta$ -syn  
209 overexpression, but instead, as previously observed after ICV injection of AAV (Figure 1B),  
210 the disease appeared significantly earlier in the AAV $\beta$ -syn injected mice as compared to  
211 control AAVGFP animals ( $p < 0,001$ ) (Figure 5E). As in previous experiments, no impact was  
212 found on the  $\alpha$ -syn<sup>P</sup> levels even if  $\beta$ -syn was significantly increased at the stage of clinical  
213 signs in all the CNS regions (Figure 5D, F).

214 By immunohistochemistry, as with the low dose of AAV, a specific  $\beta$ -syn staining punctate  
215 pattern was detected in the inoculated mesencephalon, as well as in the striatum and brain

216 stem in two sick M83 mice inoculated with AAV $\beta$ -syn, but not in one mouse inoculated with  
217 AAVGFP (data not shown).

218

### 219 **AAV-mediated overexpression of $\beta$ -syn might have formed aggregates of $\beta$ -syn**

220 Proteinase K (PK)-resistant  $\beta$ -syn aggregates have been previously described after inoculation  
221 of AAV vectors expressing human  $\beta$ -syn in the *substantia nigra* of rats<sup>10,11</sup>. We thus analyzed  
222 by immunohistochemistry the brain of several sick M83 mice after inoculation of AAVs in  
223 the VTA (Figure 6). After PK digestion, total  $\beta$ -syn antibody revealed a punctate pattern  
224 specifically detected after the inoculation of AAV $\beta$ -syn, in the mesencephalon of 7/7 sick  
225 M83 mice (5 mice injected with low dose of AAV, of which 2 were challenged with  
226 M83/M83 inoculum and 3 with MSA/M83 inoculum, as well as 2 mice injected with high  
227 dose of AAV and challenged with M83/M83 inoculum). This punctate pattern was also  
228 detected in the striatum and the brain stem where the AAV is also expressed, but not in the  
229 cerebellum where the AAV is less expressed (Supplementary figure 4). A few cell bodies  
230 were also stained with total  $\beta$ -syn antibody after PK digestion, particularly in the  
231 mesencephalon of these mice (data not shown). Even if diffuse, PK resistant staining was also  
232 detected in the hippocampal region of two sick M83 mice injected with AAV $\beta$ -syn and not  
233 challenged with brain extract inoculation, but not in one sick M83 control mouse (data not  
234 shown). These results confirm that overexpression of  $\beta$ -syn resulted in PK-resistant  $\beta$ -syn  
235 staining which could be detected independently of the vector dose, the inoculation site or the  
236 age of inoculation. Interestingly, Western blot detection of  $\beta$ -syn in the brain homogenates  
237 from sick M83 mice injected with high dose of AAV $\beta$ -syn showed the appearance of an  
238 additional band, consistent with a dimer, that is not visible in the homogenates from sick M83  
239 mice injected or not with AAVGFP (even after long exposure of the blot) (Supplementary  
240 figure 5).

241

242 **Discussion**

243  $\beta$ -syn was previously described as a neuroprotective protein, able to inhibit the aggregation  
244 process of  $\alpha$ -syn *in vitro* and having benefic effects on synucleinopathies *in vivo*<sup>6-9,15</sup>. Here,  
245 we tried to slow down a synucleinopathy in a transgenic mouse model with dramatic clinical  
246 symptoms linked to pathological  $\alpha$ -syn aggregation. In particular, we analyzed the effects of  
247 the overexpression of  $\beta$ -syn mediated by an AAV vector on  $\alpha$ -syn aggregation. We show here  
248 that the delivery of the AAV $\beta$ -syn vector *via* two different injection routes  
249 (intracerebroventricular or in the ventral tegmental area) in transgenic M83 mice, neither  
250 delayed the disease onset nor reduced the levels of pathological  $\alpha$ -syn at the disease stage,  
251 despite a sustained overexpression of  $\beta$ -syn. A limitation of our study remains the low number  
252 of animals that were followed in each of the experimental groups, given the multiple  
253 strategies that were studied (different routes and ages of AAV inoculations, different AAV  
254 doses, AAV effects during normal aging or after intracerebral experimental challenges of two  
255 M83 sources (M83/M83 or MSA/M83) as summarized in supplementary Table 1. This  
256 represents a statistical limitation of our study, although it is noteworthy that in the only two  
257 experimental groups in which a statistically significant difference was found between the  
258 survival of mice injected with AAV $\beta$ -syn and AAVGFP vectors, this rather suggested a  
259 deleterious effect of  $\beta$ -syn overexpression. Studies on larger cohorts will thus be required to  
260 confirm our results. A previous study indeed suggested that constitutive overexpression of  $\beta$ -  
261 syn in transgenic M83 mice by generating double transgenic mice delays the M83 disease  
262 onset by several months<sup>9</sup>. In our study, interestingly, M83 mice overexpressing  $\beta$ -syn showed  
263 a higher spontaneous activity in experiments in which open field was performed and a  
264 tendency to have more balance trouble in beam walking test (Supplementary figure 6). These  
265 results suggest that  $\beta$ -syn expression might have an impact on mice behavior without

266 affecting the ultimate development of the disease. Importantly, in this study of Fan and  
267 colleagues, human  $\beta$ -syn was expressed from the pan-neuronal mouse prion promoter, which  
268 is the same promoter used to express human mutated  $\alpha$ -syn in the M83 model. It is possible  
269 that the strategies used in our study did not provide sufficient expression of  $\beta$ -syn, in the CNS  
270 regions targeted by the disease. Indeed, as expected, after the injection of AAV in the VTA,  
271 we obtained a very high overexpression of  $\beta$ -syn in the mesencephalon in which the  
272 aggregation of  $\alpha$ -syn is high at the disease stage, but this region may not be the region where  
273 the aggregation process of  $\alpha$ -syn begins<sup>16</sup>. It should be emphasized that the major signs of the  
274 clinical disease of M83 mice are in relation with some - still poorly explained- disorders in the  
275 spinal cord<sup>17</sup>. In an additional series of experiments, we were unable to identify a  
276 degeneration of motor neurons in the lumbar spinal cord after the injection of preformed  
277 fibrils of human  $\alpha$ -syn in M83 mice, as previously reported after intra-muscular injections<sup>17</sup>,  
278 further interrogating the cause of the appearance of symptoms (Supplementary figure 7). The  
279 ICV injection of AAV9 vector in SMN $\Delta$ 7 mice, a severe model of spinal muscular atrophy,  
280 allowed to express a codon-optimized human SMN1 coding sequence in the spinal cord,  
281 which as a result, has improved significantly their survival<sup>18</sup>. After the ICV inoculation of  
282 AAV  $\beta$ -syn, the overexpression of  $\beta$ -syn was diffuse and lower in caudal regions of the brain  
283 and spinal cord, as described<sup>14</sup>, but it may have been insufficient to slow down the  
284 synucleinopathy process. It must however be noted that an *in vitro* study using AAV vectors  
285 suggests that  $\beta$ -syn overexpression is benefic on  $\alpha$ -syn linked toxicity only at a low ratio of  $\beta$ -  
286 syn/ $\alpha$ -syn expression<sup>10</sup>. Even if it was not evaluated here, another study has described  
287 transgene expression in the neuromuscular junction after AAV injection into the ventricles at  
288 birth; this may be important since the degeneration of the neuromuscular junction was also  
289 described as a possible explanation of the appearance of symptoms in M83 mice<sup>14,17</sup>. At the  
290 cellular level, human  $\beta$ -syn seems mostly localized in the presynaptic button and axons in sick

291 M83 mice, which seems appropriate because the aggregation of  $\alpha$ -syn was suggested to start  
292 at the presynaptic level in synucleinopathies<sup>19,20</sup>. Another study suggested that the benefic  
293 effect of  $\beta$ -syn is the result of the down regulation of the expression of  $\alpha$ -syn, but we did not  
294 detect any decrease of  $\alpha$ -syn expression, even in the brain regions overexpressing  $\beta$ -syn (data  
295 not shown). In another transgenic mouse model (D line) overexpressing human wild type  $\alpha$ -  
296 syn, two studies reported the reduction of the synucleinopathy by either generating bigenic  
297 mice that also overexpress  $\beta$ -syn, or vehiculating the human  $\beta$ -syn transgene, under the  
298 control of cytomegalovirus (CMV) promoter, in a lentiviral vector<sup>7,8</sup>. As some reports  
299 indicate a downregulation of the CMV promoter in the CNS over time<sup>21</sup>, we chose here to  
300 use the human synapsin 1 promoter to obtain a long term expression of  $\beta$ -syn, which was  
301 confirmed in the present study, even in old mice. Importantly, as previously described<sup>22</sup>, the  
302 synapsin 1 promoter also allowed to express human  $\beta$ -syn specifically in neurons, where  $\alpha$ -  
303 syn aggregates are found in the M83 model<sup>1</sup>. According to the study by Hashimoto *et al.*, the  
304 neuroprotective effect of  $\beta$ -syn was associated to the activation of Akt, a neuroprotective  
305 protein which could be indirectly down-regulated by  $\alpha$ -syn during the synucleinopathy  
306 process<sup>23</sup>. However, we did not detect any significant increase of Akt activation by Western  
307 blot in 6 months-old M83 mice inoculated with AAV $\beta$ -syn in the VTA at 2 months, and  
308 challenged one month later with the M83/M83 inoculum (Supplementary figure 8). It should  
309 be noticed that such Akt changes were not consistently observed, as shown in a study with a  
310 lentiviral vector used for  $\beta$ -syn overexpression<sup>24</sup>.

311 Surprisingly, in the present study, two experiments in mice challenged with a M83/M83  
312 inoculum rather showed a significant acceleration of the disease after AAV  $\beta$ -syn injection  
313 (Fig 1B and 5E). Interestingly, several studies reported that  $\beta$ -syn could be implicated in the  
314 pathological process of synucleinopathies. Indeed, an axonal pathology with  $\beta$ -syn  
315 accumulation in axons was reported in patients with Parkinson's disease, DLB or

316 Hallervorden-Spatz syndrome <sup>25,26</sup>. In addition, two mutations of  $\beta$ -syn, identified in DLB  
317 cases, were suggested to be responsible for  $\alpha$ -syn aggregation and DLB <sup>27</sup>. Generating  
318 transgenic mice co-expressing P123H mutated  $\beta$ -syn with human  $\alpha$ -syn resulted in an  
319 enhanced pathology, suggesting that mutated  $\beta$ -syn could potentiate  $\alpha$ -syn aggregation <sup>28</sup>.  
320 Variable results were also observed after overexpression of  $\beta$ -syn using a lentiviral vector  
321 after inoculation into the hippocampus of transgenic mice overexpressing a mutated form of  
322 the human  $\beta$ -amyloid precursor protein (APP) involved in Alzheimer's disease, as assessed by  
323 examining plaque load, memory deficits, and anxiety <sup>24</sup>. However, it should be noted that the  
324 expression level of  $\beta$ -syn was relatively low in this latter study (not detectable at the protein  
325 level). Also, it is interesting to notice that a truncated form of human recombinant  $\alpha$ -syn  
326 lacking the 71-82 residues not able to form aggregates *in vitro*, like  $\beta$ -syn <sup>29</sup>, accelerated the  
327 disease of a few M83 mice, after injection in the muscle or in the peritoneal cavity <sup>17,30</sup>. These  
328 results raise the possibility that  $\beta$ -syn might be able to accelerate the aggregation of  $\alpha$ -syn in  
329 M83 mice, although this has not been reported so far.

330 Further analyzing the effects of  $\beta$ -syn expression in sick M83 mice inoculated with the AAV  
331 vector in the VTA allowed detecting a punctate pattern of  $\beta$ -syn staining in the targeted brain  
332 region and some connected regions, only in mice inoculated with AAV $\beta$ -syn. This staining  
333 was more resistant to PK digestion than that endogenous  $\beta$ -syn in control mice. This result  
334 suggests that overexpressed  $\beta$ -syn formed aggregates which could explain why  $\beta$ -syn did not  
335 act as expected, *i.e* as an  $\alpha$ -syn aggregation inhibitor. Landeck *et al.* have described the same  
336 staining of  $\beta$ -syn resistant to PK digestion referred as "dark punctae", two months after the  
337 inoculation of AAV5 carrying human  $\beta$ -syn under the control of chicken beta-actin promoter  
338 including a CMV enhancer element (CBA) in the *substantia nigra* of rats <sup>11</sup>. Before this study,  
339 Taschenberger *et al.* have also described the detection of PK-resistant  $\beta$ -syn aggregates *in*  
340 *vivo*, as early as two weeks following the inoculation of AAV2 carrying human  $\beta$ -syn gene in

341 the *substantia nigra* of rats<sup>10</sup>. This time, the vector design was closer to ours, using the same  
342 promoter (human synapsin) to express human  $\beta$ -syn, with a WPRE sequence to enhance  
343 transgene expression. It is interesting to notice that, even if the AAV serotype used as well as  
344 the vector design can differ between studies, all these studies that used AAV to carry  $\beta$ -syn  
345 also reported the detection of  $\beta$ -syn aggregates. Furthermore, our observations in  
346 immunohistochemistry are supported biochemically in the present study, by the detection of a  
347 specific  $\beta$ -syn pattern in Western blot that could be a specific signature of  $\beta$ -syn aggregation,  
348 in mice showing overexpression of  $\beta$ -syn after injection of high dose of AAV $\beta$ -syn  
349 (Supplementary figure 5). All these observations suggest that the neuroprotective effect of  $\beta$ -  
350 syn may vary according to the strategy followed to overexpress it and the animal model. For  
351 example, it would be interesting to inject AAV vectors used in this study in transgenic D mice  
352 in order to see if we obtain the same  $\beta$ -syn aggregates. The D line is indeed an example of  
353 transgenic mice expressing the normal human  $\alpha$ -syn, which may thus be more representative  
354 of the common situation in humans. The interest of the M83 mouse line, which is well  
355 illustrated in our study, is the possibility to easily quantify both survival of mice, ultimately  
356 showing a major clinical disease, and levels of pathological  $\alpha$ -syn, using an ELISA test. The  
357 A53T mutation in the human protein is however associated with a high propensity to  
358 aggregation<sup>31</sup> and our observations with AAV-mediated  $\beta$ -syn overexpression may not be  
359 representative of the situation of humans with non genetic synucleinopathies. Also, it is  
360 important to point out that even if most of neurons express the transgene in the cerebral region  
361 injected of mice in our study, there is an important variability of the expression of the  
362 transgene in transduced cells after AAV vectors injection (Supplementary figure 9). It might  
363 explain at least partly the difficulty to detect a benefic effect of  $\beta$ -syn overexpression as it was  
364 suggested to depend on a specific  $\alpha$ -syn/ $\beta$ -syn ratio in cell culture<sup>10</sup>.

365 The present study suggest for the first time that  $\beta$ -syn overexpression could not be benefic in a  
366 synucleinopathy model. This may be due at least partly to the formation of a PK-resistant  $\beta$ -  
367 syn species after AAV $\beta$ -syn inoculation. According to a very recent study, a mildly acidic pH  
368 environment, found in several organelles, could induce  $\beta$ -syn aggregation, highlighting the  
369 complexity of  $\beta$ -syn fibrillation mechanisms occurring *in vivo*<sup>32</sup>. Further studies are needed to  
370 better understand how and to what extent  $\beta$ -syn could play a role in synucleinopathies.

371 However, even though we could not detect any protective effects of  $\beta$ -syn, our study confirms  
372 that an AAV vector is suitable for long-term overexpression of proteins into the CNS.  
373 Notably, after ICV inoculations of AAV in neonates, we confirmed a widespread expression  
374 of the protein, as this was also recently described using an  $\alpha$ -syn AAV vector<sup>33</sup>. The injection  
375 of AAV in the VTA also allowed to express human  $\beta$ -syn in various connected regions, as  
376 suggested in a previous study using serotype 9 AAV vector carrying a lysosomal enzyme  
377 gene<sup>13</sup>. Our data also illustrate the robustness of the experimental model of M83 mice  
378 intracerebrally challenged by inocula containing aggregated  $\alpha$ -syn, showing rather short and  
379 relatively uniform survival periods before the appearance of characteristics clinical signs,  
380 which can be used for the assessment of future therapeutic strategies.

381

## 382 **Methods**

383 *Animals:* M83 transgenic mice were used in this study (B6;C3H-Tg[SNCA]83Vle/J,  
384 RRID:MGI:3603036, The Jackson Laboratory, Bar Harbor, ME, USA). These mice express  
385 A53T mutated human  $\alpha$ -syn protein and spontaneously develop severe motor impairment  
386 leading to early death<sup>1</sup>. Homozygous M83 mice develop characteristic motor symptoms  
387 between 8 and 16 months of life, beginning with reduced ambulation, balance disorders,  
388 partial paralysis of a hind leg and then progressing to prostration, difficulty in feeding, weight  
389 loss, hunched back and general paralysis<sup>1</sup>. The animals were housed per group in enriched

390 cages in a temperature-controlled room on a 12h light/dark cycle, and received water and food  
391 *ad libitum*, in our approved facilities (No. C69 387 0801) for breeding and experimental  
392 studies, in accordance with EEC Directive 86/609/EEC and French decree No. 2013-118. The  
393 experimental studies described in this article were performed in containment level 3 facilities  
394 and authorized by the « Comité d'éthique » CE2A – 16, ComEth ANSES/ENVA/UPEC and  
395 by the « Ministère de l'enseignement supérieur, de la recherche et de l'innovation » (ref 16-  
396 006). All experiments were performed in accordance with relevant guidelines and regulations.

397

398 *AAV vectors:* Recombinant self-complementary AAV9 vectors (scAAV9) encoding human  $\beta$ -  
399 syn or enhanced GFP (eGFP) were produced by calcium phosphate transfection of HEK-293  
400 cells<sup>34</sup>. Three plasmids were transfected simultaneously: (i) a vector plasmid containing the  
401 human gene of  $\beta$ -syn or eGFP under control of the neuron-specific synapsin 1 gene promoter  
402 (Supplementary figure 1A) (ii) a helper plasmid pXX6<sup>35</sup> and (iii) a plasmid carrying rep2 and  
403 cap9 genes<sup>36</sup>. Vector particles were extracted and purified on an iodixanol step gradient.  
404 Titers were determined by quantitative polymerase chain reaction (qPCR) and expressed as  
405 viral genomes per milliliter (vg/mL).

406

407 *Inoculations:* AAV vectors were injected at birth or at adulthood (two months of age), at  
408 different sites of inoculation. Neonates were inoculated using 5  $\mu$ L Hamilton syringe, with  
409  $9.38 \times 10^8$  vg of AAV $\beta$ -syn or  $2.73 \times 10^8$  vg of AAVGFP vectors per lateral ventricle of the  
410 viral solution with 0.05% Trypan blue<sup>12</sup>. Adults mice were inoculated with  $3.75 \times 10^8$  vg of  
411 AAV $\beta$ -syn or  $1.09 \times 10^8$  vg of AAVGFP (or with high dose:  $1.5 \times 10^9$  vg of AAV $\beta$ -syn or  
412  $4.36 \times 10^8$  vg of AAVGFP) of viral solution in the ventral tegmental area located in the  
413 mesencephalon, using stereotaxic coordinates (anteroposterior: -3.16 mediolateral: +0.25  
414 dorsoventral: -4.50). Two months after the inoculation of the viral solution in neonates or one

415 month after the inoculation of the viral solution in adults, M83 mice were inoculated with  
416 brain homogenates from a second passage of a sick M83 brain sample in M83 mice  
417 (M83/M83 inoculum) or a second passage of a patient with multiple system atrophy (MSA)  
418 brain sample in M83 mice (MSA/M83 inoculum) (same sample used in a previous publication  
419 <sup>5</sup>). These homogenates were injected in the left striatum, using stereotaxic coordinates (AP:  
420 +0.14 ML: +2 DV: -2.75). Before each stereotaxic surgery (AAV or brain extract  
421 inoculation), mice have been anesthetized with a xylazine (10 mg/kg) and ketamine (100  
422 mg/kg) mixture.

423

424 *qRT-PCR*: B6C3H brains were dissected and RNA was extracted from brain regions using  
425 RNeasy lipid tissue Minikit (ref 74804, Qiagen, Courtaboeuf, France). RNA samples were  
426 tittered using Nanodrop (Nanodrop 1000, Thermo Fisher scientific, Villebon sur Yvette,  
427 France). 500 ng of RNA were reverse-transcribed with Quanta qScript cDNA Super Mix (ref  
428 95048-100, VWR international, Fontenay-sous-Bois, France) on a Biorad iCycler. After a  
429 1:10 dilution, complementary DNA samples were analyzed by qPCR using primers specific  
430 for the WPRE region of viral mRNA, and primers specific for GAPDH mRNA. We used the  
431 LC 480 SYBR Green 1 Master kit (ref 04887 352 001, Roche, Boulogne-Billancourt, France)  
432 on a Roche Light Cycler 480 to perform the qPCR and analyzed the results on the LC 480  
433 software.

434

435 *ELISA*: Brains were dissected as described <sup>4</sup> and proteins were extracted in high salt buffer  
436 (50 mM Tris-HCl, pH 7.5, 750 mM NaCl, 5 mM EDTA, 1 mM DTT, 1% phosphatase and  
437 protease inhibitor cocktails), using a mechanical homogenizer (grinding balls, Precellys 24,  
438 Bertin Technologies, Montigny-le-Bretonneux, France) to obtain a 10% homogenate (w/v).

439 Each sample was titered using the DC<sup>TM</sup> protein assay kit (ref 5000111, Biorad, Marnes-la-  
440 Coquette, France).

441 As already described for  $\alpha$ -syn<sup>P</sup> detection <sup>3,5</sup>, plates were saturated with Superblock T20  
442 (Thermo Scientific, Rockford, IL, USA) for 1 h at 25°C, under agitation (150 rpm). After 5  
443 washes in PBST, 10  $\mu$ g of protein (for  $\alpha$ -syn<sup>P</sup> detection) diluted in PBST were incubated for 2  
444 h at 25°C, under agitation (150 rpm).  $\alpha$ -syn<sup>P</sup> was detected with a rabbit polyclonal antibody  
445 against P<sup>Ser129</sup>  $\alpha$ -syn (ref ab59264, Cambridge, UK) diluted to 1:3,000 in PBST with 1%  
446 bovine serum albumin (BSA); plates were incubated for 1 h at 25°C under agitation. After 5  
447 washes, anti-rabbit IgG HRP conjugate (ref 4010-05, SouthernBiotech, Birmingham, AL,  
448 USA) was added at 1:2,000 (for  $\alpha$ -syn<sup>P</sup> detection). After washing, 100  $\mu$ L of 3,3',5,5'-  
449 tetramethylbenzidine solution (ref. T0440, Sigma, Saint-Quentin-Fallavier, France) were  
450 added to each well and plates were incubated for 15 min with shaking. The reaction was  
451 stopped with 100  $\mu$ L of 1 N HCl, and the absorbance was measured at 450 nm with the  
452 microplate reader Model 680 (Clariostar, BMG Labtech, Champigny sur Marne, France).

453 ELISA allowing total  $\beta$ -syn quantification was adapted based on an ELISA already published  
454 <sup>24</sup>. Briefly, 2  $\mu$ g or 0.2  $\mu$ g (for Figure 5) of brain homogenate was diluted in carbonate-  
455 bicarbonate buffer 50mM (pH 9.6) and incubated at 4°C overnight. After 5 washes in PBST,  
456 plates were saturated with Superblock T20 for 1 h at 25°C, under agitation (150 rpm). After 5  
457 washes in PBST, plates were incubated with 1:2,000 of an anti- $\beta$ -syn antibody ab76111 (ref  
458 EP1537Y, Abcam, Cambridge, UK). After 5 washes in PBST, plates were incubated with an  
459 anti-rabbit IgG HRP conjugate (ref 4010-05, SouthernBiotech, Birmingham, AL, USA) at  
460 1:4,000. After washing, immunoreactivity was revealed with the same protocol as for  $\alpha$ -syn  
461 ELISA.

462

463 *Western blot:* 50 µg (for phosphorylated Akt detection) or 10 µg of proteins (for total Akt  
464 detection) or 2 µg of proteins (for GFP and β-syn detection) were separated in 12% SDS-  
465 polyacrylamide gels and electroblotted onto polyvinylidene fluoride (PvF) membranes 0,45  
466 µm (Bio-Rad). The membranes were washed 3 times in Tris-Buffered Saline (TBS) for 5 min  
467 at room temperature (RT) under agitation and were saturated 1 h with 5% BSA in TBS 0.1%  
468 Tween20 (TBST). Membranes were incubated with rabbit antibody against phosphorylated  
469 Akt at Ser473 (ref 9271S, Ozyme, Montigny-le-Bretonneux, France) at 1:1,000 or with rabbit  
470 antibody against total Akt (ref 9272, Ozyme, Montigny-le-Bretonneux, France) at 1:1,000 or  
471 with anti-β-syn antibody ab76111 (ref EP1537Y, Abcam, Cambridge, UK) at 1:5,000 or with  
472 anti-GFP antibody (ref ab290, Abcam, Cambridge, UK) at 1:1,000 or with anti-β-actin  
473 antibody (ref ab8226, Abcam, Cambridge, UK) at 1:2000 overnight at 4°C. After 3 washes,  
474 the membranes were incubated for 1 h at RT with anti-rabbit HRP-linked antibody (ref  
475 7074P2, Ozyme, Montigny-le-Bretonneux, France) for detection of total Akt and  
476 phosphorylated Akt at 1:2,000, or with anti-rabbit HRP-linked antibody (ref 4010-05,  
477 SouthernBiotech, Birmingham, AL, USA). The immunocomplexes were revealed with  
478 chemiluminescent reagents (Supersignal WestDura, ref 34076, Pierce, Interchim, MontLuçon,  
479 France), and analyzed using the ChemiDoc system (Bio-Rad) and Image Lab software (Bio-  
480 Rad) which allowed to quantify the intensity of the bands.

481

482 *Immunohistochemistry/Immunofluorescence:* After dissection, brain samples were fixed in 4%  
483 paraformaldehyde and paraffin embedded to be cut into serial 6 µm sections. After  
484 deparaffinization, endogeneous peroxidase activity was directly blocked with oxygenated  
485 water 3% during 5 minutes at RT. Brain sections were pretreated with a citrate solution (ref  
486 C9999, Sigma, Saint-Quentin-Fallavier, France) with heat antigen retrieval. For the detection  
487 of α-syn phosphorylated at serine 129 by immunohistochemistry, we did an additional antigen

488 retrieval step in which sections were treated with a 4 M solution of guanidinium thiocyanate  
489 during 20 min. After washing, sections were saturated using a blocking reagent (ref  
490 11096176001, Roche), 1 h at RT and incubated with antibody against  $\beta$ -syn ab76111 in PBST  
491 (ref EP1537Y, Abcam, Cambridge, UK) diluted at 1:500, anti-synaptophysin antibody SY38  
492 (ref ab8049, Abcam, Cambridge, UK) diluted at 1:10 or anti-GFP antibody (ref ab290,  
493 Abcam, Cambridge, UK) diluted at 1:500 or anti-tubulin  $\beta$ -3 antibody (ref MMS-435P,  
494 Biologend, San diego, USA) diluted at 1:100) at 4°C overnight. For the detection  
495 phosphorylated at S129  $\alpha$ -syn we used a rabbit antibody (ref: ab51253, Abcam, Cambridge,  
496 GB) diluted at 1:300 in TBST for immunohistochemistry, and a mouse antibody (ref:  
497 pSyn#64, FUJIFILM Wako Pure Chemical Corporation, China) diluted at 1:1000 in TBST for  
498 immunofluorescence analysis (with the rabbit anti- $\beta$ -syn antibody, Supplementary figure 3),  
499 at 4°C overnight. After another blocking step 30 minutes at RT, for immunohistochemistry,  
500 sections were incubated 1 h at RT with anti-rabbit IgG HRP conjugate (ref 4010-05,  
501 SouthernBiotech, Birmingham, AL, USA) diluted at 1:250 in PBST or TBST. Antibody  
502 binding was detected using DAB peroxidase substrate (ref SK-4100, Vector Laboratories,  
503 Burlingame, CA USA) intensified with nickel chloride for  $\beta$ -syn or ImmPACT DAB  
504 peroxidase (HRP) substrate (ref SK-4105, Vector Laboratories, Burlingame, CA USA) for  
505 phosphorylated  $\alpha$ -syn detection. For immunofluorescence, sections were incubated 1 h at RT  
506 with anti-rabbit IgG AlexaFluor 488 or 555 (ref A-11008 and ref A21428, respectively,  
507 Thermofischer scientific, Villebon sur Yvette, France) or with anti-mouse IgG AlexaFluor  
508 488 or 555 (ref A11001 and A21127 respectively, Thermofischer scientific, Villebon sur  
509 Yvette, France) diluted at 1:1000. After washings in PBST then in PBS, sections were treated  
510 with an autofluorescence eliminator reagent (ref 2160, Millipore, Temecula, USA), before  
511 mounting.

512

513 *PK digestion:* After being deparaffinized, sections were incubated with a 10 µg/mL solution  
514 of proteinase K (ref EU0090-B, Euromedex, Souffelweyersheim, France) diluted in PBS, 10  
515 minutes at RT (protocol adapted from <sup>10</sup>). Sections were washed three times in water before  
516 blocking the endogenous peroxidase activity and pursuing the immunohistochemistry staining  
517 protocol.

518

519 *Statistical analysis:* Survival time was defined as the time from birth until death (Figure 3A,  
520 exclusively) or as the time from the inoculation of the brain extract until the appearance of the  
521 first specific M83 symptoms and euthanasia of the mouse. The detection of these specific  
522 symptoms was done blindly with regard to the initial AAV (β-syn or GFP) treatment. We  
523 right-censored mice found dead without M83 disease identification. Survival times were  
524 compared using log-rank test. Concerning statistical analysis of ELISA tests results, means  
525 were compared using Wilcoxon test. The difference was significant when  $p < 0,05$  (\*),  
526  $p < 0,01$ (\*\*),  $p < 0,001$ (\*\*\*).

527

## 528 **Acknowledgements**

529 We are grateful to Eric Morignat and Habiba Tlili for their help and advices on statistical and  
530 immunofluorescence assays, respectively. We also are grateful for Olivier Biondi for its help  
531 setting up behavioral test and the method for quantifying motor neurons in the spinal cord.  
532 We thank Ronald Melki and its team for providing us preformed fibrils of recombinant α-syn.  
533 This research was partly funded by the Fondation France Parkinson. D.S was supported by  
534 funds from the Région Auvergne-Rhône-Alpes – ARC1 Santé.

535

## 536 **Author contributions**

537 DS, DB, MD, DG, performed experiments. JV, JNA contributed to biochemical and  
538 immunohistochemistry assays respectively. LL supervised animal experiments in containment  
539 level 3 facilities. AS supervised all the construction and the production of viral vectors. TB,  
540 DB designed experiments and supervised the study. DS, TB, DB, AS wrote the paper. All  
541 authors read and approved the final manuscript.

542

### 543 **Conflicts of interest**

544 The authors declare that they have no competing interests.

545

### 546 **REFERENCES**

547

- 548 1 Giasson, B. I. *et al.* Neuronal alpha-synucleinopathy with severe movement disorder in mice  
549 expressing A53T human alpha-synuclein. *Neuron* **34**, 521-533, doi:10.1016/S0896-  
550 6273(02)00682-7 (2002).
- 551 2 Mougenot, A. L. *et al.* Prion-like acceleration of a synucleinopathy in a transgenic mouse  
552 model. *Neurobiology of aging* **33**, 2225-2228, doi:10.1016/j.neurobiolaging.2011.06.022  
553 (2012).
- 554 3 Betemps, D. *et al.* Alpha-synuclein spreading in M83 mice brain revealed by detection of  
555 pathological alpha-synuclein by enhanced ELISA. *Acta Neuropathologica Communications* **2**,  
556 29, doi:10.1186/2051-5960-2-29 (2014).
- 557 4 Betemps, D. *et al.* Detection of Disease-associated alpha-synuclein by Enhanced ELISA in the  
558 Brain of Transgenic Mice Overexpressing Human A53T Mutated alpha-synuclein. *Journal of*  
559 *visualized experiments : JoVE*, e52752, doi:10.3791/52752 (2015).
- 560 5 Sargent, D. *et al.* 'Prion-like' propagation of the synucleinopathy of M83 transgenic mice  
561 depends on the mouse genotype and type of inoculum. *Journal of neurochemistry* **143**, 126-  
562 135, doi:10.1111/jnc.14139 (2017).
- 563 6 Janowska, M. K., Wu, K. P. & Baum, J. Unveiling transient protein-protein interactions that  
564 modulate inhibition of alpha-synuclein aggregation by beta-synuclein, a pre-synaptic protein  
565 that co-localizes with alpha-synuclein. *Scientific Reports* **5**, 15164, doi:10.1038/srep15164  
566 (2015).
- 567 7 Hashimoto, M. *et al.* An antiaggregation gene therapy strategy for Lewy body disease  
568 utilizing beta-synuclein lentivirus in a transgenic model. *Gene therapy* **11**, 1713-1723,  
569 doi:10.1038/sj.gt.3302349 (2004).
- 570 8 Hashimoto, M., Rockenstein, E., Mante, M., Mallory, M. & Masliah, E. beta-Synuclein inhibits  
571 alpha-synuclein aggregation: a possible role as an anti-parkinsonian factor. *Neuron* **32**, 213-  
572 223 (2001).
- 573 9 Fan, Y. *et al.* Beta-synuclein modulates alpha-synuclein neurotoxicity by reducing alpha-  
574 synuclein protein expression. *Human molecular genetics* **15**, 3002-3011,  
575 doi:10.1093/hmg/ddl242 (2006).

- 576 10 Taschenberger, G. *et al.* beta-synuclein aggregates and induces neurodegeneration in  
577 dopaminergic neurons. *Annals of neurology* **74**, 109-118, doi:10.1002/ana.23905 (2013).
- 578 11 Landeck, N., Buck, K. & Kirik, D. Toxic effects of human and rodent variants of alpha-synuclein  
579 in vivo. *The European journal of neuroscience* **45**, 536-547, doi:10.1111/ejn.13493 (2017).
- 580 12 Kim, J. Y., Grunke, S. D., Levites, Y., Golde, T. E. & Jankowsky, J. L. Intracerebroventricular  
581 viral injection of the neonatal mouse brain for persistent and widespread neuronal  
582 transduction. *Journal of visualized experiments : JoVE*, 51863, doi:10.3791/51863 (2014).
- 583 13 Cearley, C. N. & Wolfe, J. H. A single injection of an adeno-associated virus vector into nuclei  
584 with divergent connections results in widespread vector distribution in the brain and global  
585 correction of a neurogenetic disease. *The Journal of neuroscience : the official journal of the*  
586 *Society for Neuroscience* **27**, 9928-9940, doi:10.1523/jneurosci.2185-07.2007 (2007).
- 587 14 McLean, J. R. *et al.* Widespread neuron-specific transgene expression in brain and spinal cord  
588 following synapsin promoter-driven AAV9 neonatal intracerebroventricular injection.  
589 *Neuroscience letters* **576**, 73-78, doi:10.1016/j.neulet.2014.05.044 (2014).
- 590 15 Hashimoto, M. *et al.* Beta-synuclein regulates Akt activity in neuronal cells. A possible  
591 mechanism for neuroprotection in Parkinson's disease. *The Journal of biological chemistry*  
592 **279**, 23622-23629, doi:10.1074/jbc.M313784200 (2004).
- 593 16 Emmer, K. L., Waxman, E. A., Covy, J. P. & Giasson, B. I. E46K human alpha-synuclein  
594 transgenic mice develop Lewy-like and tau pathology associated with age-dependent,  
595 detrimental motor impairment. *The Journal of biological chemistry* **286**,  
596 doi:10.1074/jbc.M111.247965 (2011).
- 597 17 Sacino, A. N. *et al.* Intramuscular injection of alpha-synuclein induces CNS alpha-synuclein  
598 pathology and a rapid-onset motor phenotype in transgenic mice. *Proceedings of the*  
599 *National Academy of Sciences of the United States of America* **111**, 10732-10737,  
600 doi:10.1073/pnas.1321785111 (2014).
- 601 18 Armbruster, N. *et al.* Efficacy and biodistribution analysis of intracerebroventricular  
602 administration of an optimized scAAV9-SMN1 vector in a mouse model of spinal muscular  
603 atrophy. *Molecular Therapy. Methods & Clinical Development* **3**, 16060,  
604 doi:10.1038/mtm.2016.60 (2016).
- 605 19 Schulz-Schaeffer, W. J. The synaptic pathology of alpha-synuclein aggregation in dementia  
606 with Lewy bodies, Parkinson's disease and Parkinson's disease dementia. *Acta*  
607 *neuropathologica* **120**, 131-143, doi:10.1007/s00401-010-0711-0 (2010).
- 608 20 Spinelli, K. J. *et al.* Presynaptic alpha-synuclein aggregation in a mouse model of Parkinson's  
609 disease. *The Journal of neuroscience : the official journal of the Society for Neuroscience* **34**,  
610 2037-2050, doi:10.1523/jneurosci.2581-13.2014 (2014).
- 611 21 Gray, S. J. *et al.* Optimizing promoters for recombinant adeno-associated virus-mediated  
612 gene expression in the peripheral and central nervous system using self-complementary  
613 vectors. *Human gene therapy* **22**, 1143-1153, doi:10.1089/hum.2010.245 (2011).
- 614 22 Glover, C. P., Bienemann, A. S., Heywood, D. J., Cosgrave, A. S. & Uney, J. B. Adenoviral-  
615 mediated, high-level, cell-specific transgene expression: a SYN1-WPRE cassette mediates  
616 increased transgene expression with no loss of neuron specificity. *Molecular therapy : the*  
617 *journal of the American Society of Gene Therapy* **5**, 509-516, doi:10.1006/mthe.2002.0588  
618 (2002).
- 619 23 Chung, J. Y. *et al.* Direct interaction of alpha-synuclein and AKT regulates IGF-1 signaling:  
620 implication of Parkinson disease. *Neurosignals* **19**, 86-96, doi:10.1159/000325028 (2011).
- 621 24 Krassnig, S. *et al.* Influence of Lentiviral beta-Synuclein Overexpression in the Hippocampus  
622 of a Transgenic Mouse Model of Alzheimer's Disease on Amyloid Precursor Protein  
623 Metabolism and Pathology. *Neuro-degenerative diseases* **15**, 243-257,  
624 doi:10.1159/000430952 (2015).
- 625 25 Galvin, J. E., Giasson, B., Hurtig, H. I., Lee, V. M. & Trojanowski, J. Q. Neurodegeneration with  
626 brain iron accumulation, type 1 is characterized by alpha-, beta-, and gamma-synuclein  
627 neuropathology. *The American journal of pathology* **157**, 361-368 (2000).

- 628 26 Galvin, J. E., Uryu, K., Lee, V. M. & Trojanowski, J. Q. Axon pathology in Parkinson's disease  
629 and Lewy body dementia hippocampus contains alpha-, beta-, and gamma-synuclein.  
630 *Proceedings of the National Academy of Sciences of the United States of America* **96**, 13450-  
631 13455 (1999).
- 632 27 Ohtake, H. *et al.* Beta-synuclein gene alterations in dementia with Lewy bodies. *Neurology*  
633 **63**, 805-811 (2004).
- 634 28 Fujita, M. *et al.* A beta-synuclein mutation linked to dementia produces neurodegeneration  
635 when expressed in mouse brain. *Nature communications* **1**, 110, doi:10.1038/ncomms1101  
636 (2010).
- 637 29 Giasson, B. I., Murray, I. V., Trojanowski, J. Q. & Lee, V. M. A hydrophobic stretch of 12 amino  
638 acid residues in the middle of alpha-synuclein is essential for filament assembly. *The Journal*  
639 *of biological chemistry* **276**, 2380-2386, doi:10.1074/jbc.M008919200 (2001).
- 640 30 Ayers, J. I. *et al.* Robust Central Nervous System Pathology in Transgenic Mice following  
641 Peripheral Injection of alpha-Synuclein Fibrils. *Journal of virology* **91**, e02095-02016,  
642 doi:10.1128/jvi.02095-16 (2017).
- 643 31 Flagmeier, P. *et al.* Mutations associated with familial Parkinson's disease alter the initiation  
644 and amplification steps of  $\alpha$ -synuclein aggregation. *Proceedings of the National Academy of*  
645 *Sciences of the United States of America* **113**, 10328-10333, doi:10.1073/pnas.1604645113  
646 (2016).
- 647 32 Moriarty, G. M. *et al.* A pH-dependent switch promotes beta-synuclein fibril formation via  
648 glutamate residues. *The Journal of biological chemistry* **292**, 16368-16379,  
649 doi:10.1074/jbc.M117.780528 (2017).
- 650 33 Delenclos, M. *et al.* Neonatal AAV delivery of alpha-synuclein induces pathology in the adult  
651 mouse brain. *Acta Neuropathologica Communications* **5**, 51, doi:10.1186/s40478-017-0455-3  
652 (2017).
- 653 34 Gao, G. P. *et al.* Novel adeno-associated viruses from rhesus monkeys as vectors for human  
654 gene therapy. *Proceedings of the National Academy of Sciences of the United States of*  
655 *America* **99**, 11854-11859, doi:10.1073/pnas.182412299 (2002).
- 656 35 Xiao, X., Li, J. & Samulski, R. J. Production of high-titer recombinant adeno-associated virus  
657 vectors in the absence of helper adenovirus. *Journal of virology* **72**, 2224-2232 (1998).
- 658 36 Gao, G. *et al.* Clades of Adeno-associated viruses are widely disseminated in human tissues.  
659 *Journal of virology* **78**, 6381-6388, doi:10.1128/jvi.78.12.6381-6388.2004 (2004).

660

661

## 662 LEGENDS

663

664 **Figure 1. Impact of the intracerebroventricular inoculation of AAV on the accelerated**  
665 **disease of M83 mice.** (A) M83 mice were injected at birth (Week 0) with AAV $\beta$ -syn or  
666 AAVGFP vectors per lateral ventricle and challenged two months later (Week 8) by the  
667 injection of M83/M83 (B-D) or MSA/M83 (E-G) inoculum in the striatum to accelerate the  
668 disease. After the appearance of the first specific symptoms of M83 disease (from 3 months to  
669 8 months after challenge), mice were sacrificed and dissected in order to perform biochemical

670 analysis. (B) M83 disease-associated survival after the inoculation of the M83/M83 brain  
671 extract is represented (significant difference according to log rank test,  $p < 0.05$ ). (C, D)  
672 Quantification of total  $\beta$ -syn (mouse  $\beta$ -syn and human  $\beta$ -syn produced by the vector) (C) or of  
673 pathological Ser129-phosphorylated form of  $\alpha$ -syn ( $\alpha$ -syn<sup>P</sup>) (D) by ELISA in CNS regions of  
674 the same sick M83 mice groups ( $n=6$  for the treated and the control group). (E) M83 disease-  
675 associated survival after the inoculation of the MSA/M83 brain extract (no significant  
676 difference according to log-rank test). (F, G) Quantification of total  $\beta$ -syn (F) or  $\alpha$ -syn<sup>P</sup> (G) by  
677 ELISA in CNS regions of the same sick M83 mice groups ( $n=6$  for the treated group and  $n=5$   
678 for the control group). Hi: hippocampus, Mes: mesencephalon, BS: brain stem, CSC: cervical  
679 spinal cord, TSC: thoracic spinal cord, LSC: lumbar spinal cord. Data are shown as mean  $\pm$   
680 sd. \* $p < 0,05$ ; \*\* $p < 0,01$ ; according to Wilcoxon test.

681

682 **Figure 2. Characterization of the AAV vectors expression after their**  
683 **intracerebroventricular inoculation in M83 mice.** M83 mice were injected with AAV  
684 vectors in the ventricles at birth and challenged with MSA/M83 inoculum (same mice than in  
685 Figure 1 E-G). (A) Detection of total  $\beta$ -syn synthesis by ELISA in cerebral regions and spinal  
686 cord of sick M83 mice 5 to 7 months after ICV injection of AAV. (B) Detection of total  $\beta$ -syn  
687 or GFP protein in the hippocampus of the same M83 mice by Western blot. Recombinant  $\beta$ -  
688 syn was loaded as a positive control. Numbers refer to each mouse ( $n=6$  in the treated group  
689 and 5 in the control group). Full blots are shown in Supplementary figure 10. (C)  
690 Quantification of total  $\beta$ -syn levels detected by WB. OB: olfactory bulbs, Cx: cerebral cortex,  
691 Str: striatum, Hi: hippocampus, Mes: mesencephalon, BS: brain stem, CSC: cervical spinal  
692 cord, TSC: thoracic spinal cord, LSC: lumbar spinal cord. Data are shown as means  $\pm$  sd.  
693 \* $p < 0,05$ ; \*\* $p < 0,01$  according to Wilcoxon test.

694

695 **Figure 3. Impact of the intracerebroventricular inoculation of AAV $\beta$ -syn or AAVGFP**  
696 **on the spontaneous M83 disease.** (A) M83 mice were injected at birth (Week 0) with  
697 AAV $\beta$ -syn or AAVGFP vectors per lateral ventricle. After the appearance of the first specific  
698 symptoms of M83 disease (from 11 months to 20 months of age), mice were sacrificed and  
699 dissected in order to perform biochemical analysis. (B) M83 disease-associated survival after  
700 the intracerebroventricular (ICV) inoculation of AAV vectors at birth (no significant  
701 difference according to log-rank test). (C, D) Quantification of total  $\beta$ -syn (B) or  $\alpha$ -syn<sup>P</sup> (C)  
702 by ELISA in CNS regions of the same sick M83 mice. No statistical analysis was done for  
703 ELISA results because the number of mice analyzed was too small (2 mice for the treated  
704 group and 3 mice for the control group). Hi: hippocampus, Mes: mesencephalon, BS: brain  
705 stem, CSC: cervical spinal cord, TSC: thoracic spinal cord, LSC: lumbar spinal cord. Data are  
706 shown as means  $\pm$  sd (n=2 and 3).

707

708 **Figure 4. Impact of the inoculation of AAV in the ventral tegmental area on M83**  
709 **disease.** (A) Two months old M83 mice (Week 8) were injected with AAV $\beta$ -syn or AAVGFP  
710 vectors in the ventral tegmental area (VTA) and challenged one month later (Week 12) by the  
711 injection of M83/M83 (B-D) or MSA/M83 (E-G) inoculum in the striatum to accelerate the  
712 disease. As before, after the appearance of the first specific symptoms of M83 disease (from 3  
713 months to 8 months after challenge), mice were sacrificed and the CNS was dissected in order  
714 to realize biochemical analysis and immunohistochemistry /immunofluorescence studies  
715 (Figure 4H, Supplementary figure 2, 3, 4). (B) M83 disease-associated survival after the  
716 inoculation of the brain extract (no significant difference according to log-rank test). (C, D)  
717 Quantification of total  $\beta$ -syn (C) or pathological Ser129-phosphorylated form of  $\alpha$ -syn ( $\alpha$ -  
718 syn<sup>P</sup>) (D) by ELISA in CNS regions of the same sick M83 mice groups (n=5 for the treated  
719 group, n=5 for the control group). (E) The M83 disease-associated survival after the

720 inoculation of the MSA/M83 inoculum (no significant difference according to log-rank test).  
721 (F, G) Quantification of total  $\beta$ -syn (F) or  $\alpha$ -syn<sup>P</sup> (G) by ELISA in CNS regions of the same  
722 mice groups (n=5 for the treated group, n=5 for the control group). (H)  
723 Immunohistochemistry pictures showing total  $\beta$ -syn staining (mouse  $\beta$ -syn and human  $\beta$ -syn  
724 produced by the vector) in the mesencephalon of 7 months old sick M83 mice inoculated with  
725 AAV  $\beta$ -syn or AAV GFP and challenged with MSA/M83 inoculum. Mes: mesencephalon,  
726 BS: brain stem, CSC: cervical spinal cord, TSC: thoracic spinal cord, LSC: lumbar spinal  
727 cord. Data are shown as means  $\pm$  sd. \*p<0,05; \*\*p<0,01 according to Wilcoxon test. Scale bar  
728 100 $\mu$ m.

729

730 **Figure 5. Characterization and impact of inoculation of AAV in the ventral tegmental**

731 **area of M83 mice.** (A-B) Two months old M83 mice were injected with AAV $\beta$ -syn or

732 AAVGFP vectors in the VTA and challenged one month later by the injection of M83/M83

733 inoculum in the striatum to accelerate the disease. In this experiment, all mice were

734 euthanized 3 months after the challenge for biochemical analysis. (A) Detection of the total  $\beta$ -

735 syn by ELISA in the brain and the spinal cord of M83 mice after inoculation of AAV $\beta$ -syn or

736 AAVGFP in the VTA (n=4 and 6, respectively). (B) Detection of  $\beta$ -syn and GFP proteins by

737 Western blot in the mesencephalon of the same sick M83 mice. Recombinant  $\beta$ -syn was

738 loaded as a positive control. Numbers refer to mice. Full blots are shown in Supplementary

739 figure 11. (C) Total  $\beta$ -syn protein quantification by ELISA test using 0,2  $\mu$ g (instead of 2  $\mu$ g)

740 of mesencephalon homogenates extracted from sick M83 mice inoculated with  $1,5 \cdot 10^9$  vg

741 (high dose, 4-times more than the low dose) or  $3,75 \cdot 10^8$  vg (low dose) of AAV $\beta$ -syn or

742 AAVGFP. These results were obtained with the same samples used in Figure 4C and 5D, but

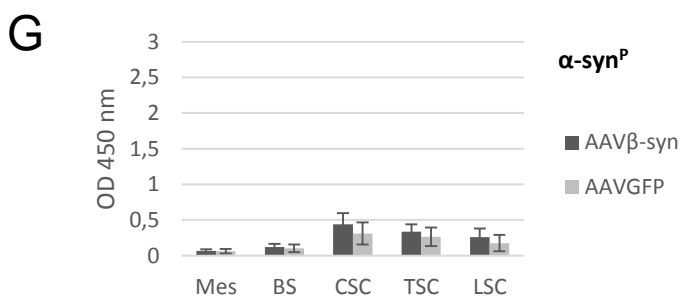
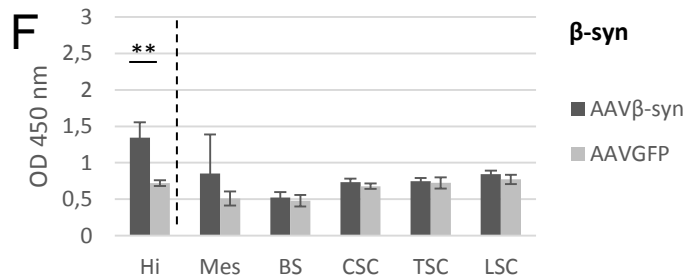
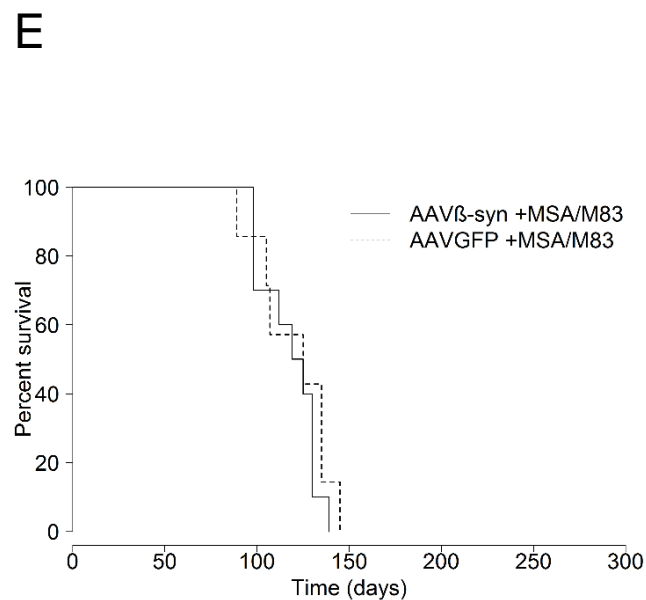
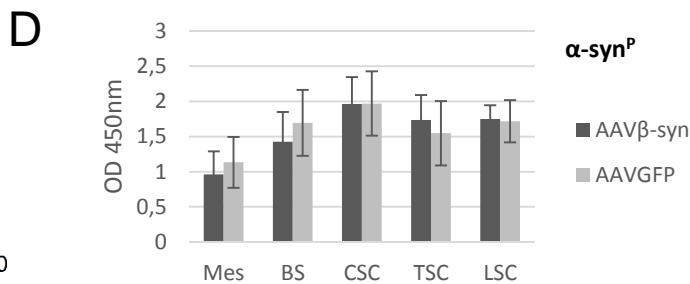
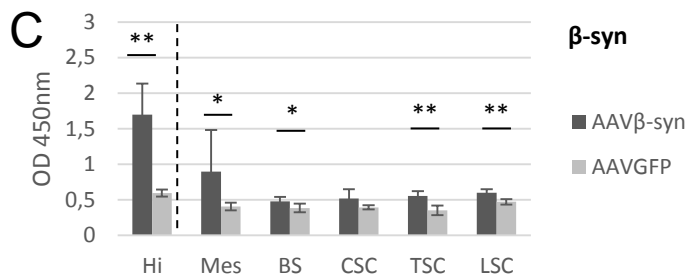
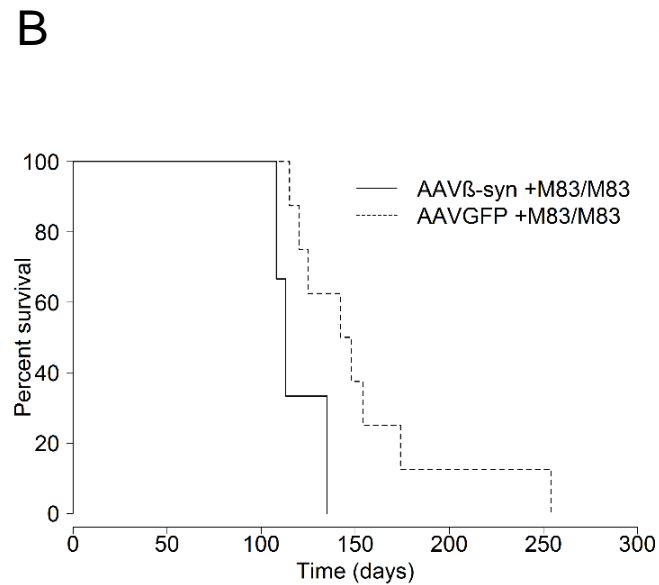
743 10 times diluted. (D-F) Two months old M83 mice (Week 8) were injected with high dose of

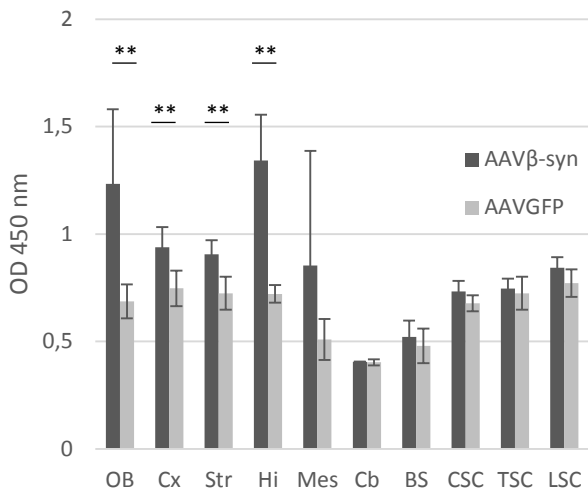
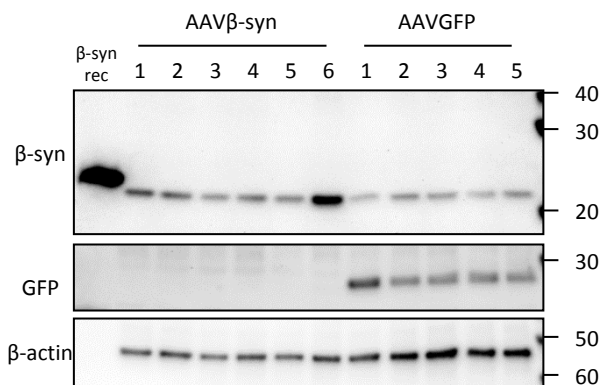
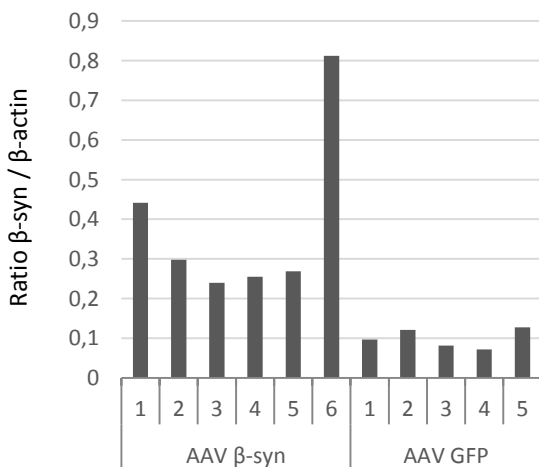
744 AAV vectors (4-times higher than in Figure 4 for each vector) in the VTA and challenged one

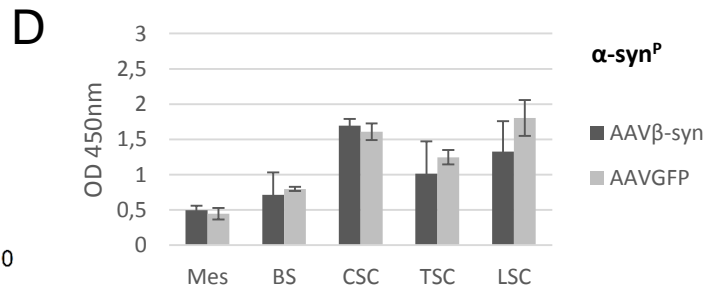
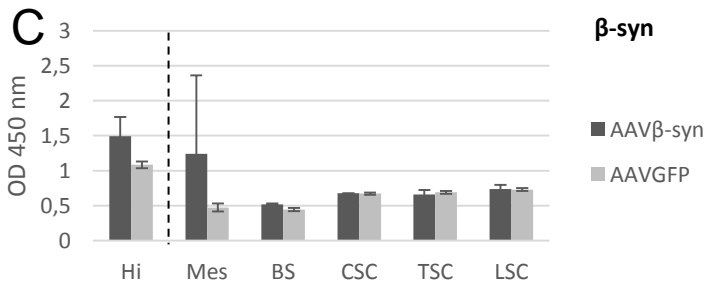
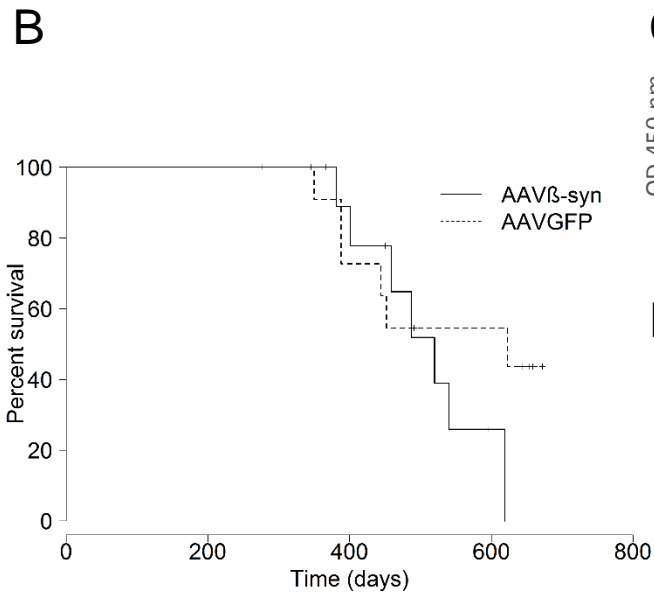
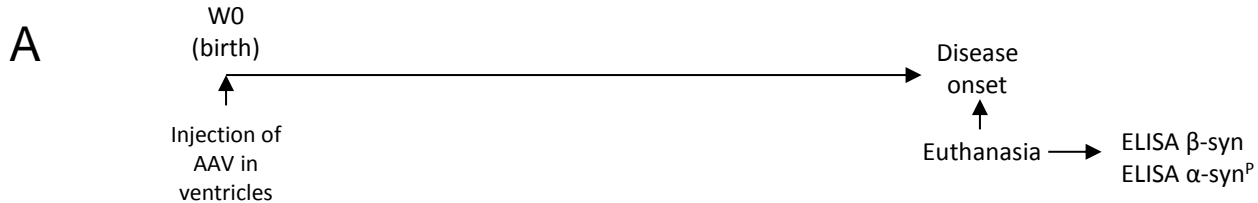
745 month later (Week 12) by injecting M83/M83 inoculum in the striatum. (D, F) Quantification  
746 of total  $\beta$ -syn (D) or  $\alpha$ -syn<sup>P</sup> (F) by ELISA in CNS regions of the same sick M83 mice groups  
747 (n=3 and 7 for the treated and control group). (E) M83 disease-associated survival after the  
748 inoculation of the brain extract (significant difference according to log-rank test,  $p < 0,001$ ).  
749 Mes: mesencephalon, BS: brain stem, CSC: cervical spinal cord, TSC: thoracic spinal cord,  
750 LSC: lumbar spinal cord. Data are shown as means  $\pm$  sd. \* $p < 0,05$ , \*\* $p < 0,01$ , according to  
751 Wilcoxon test. Scale bar 100 $\mu$ m.

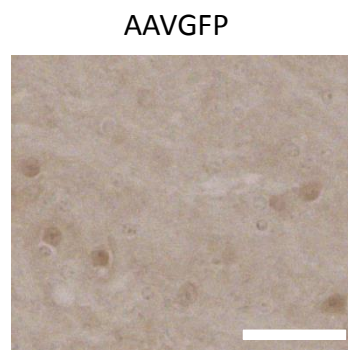
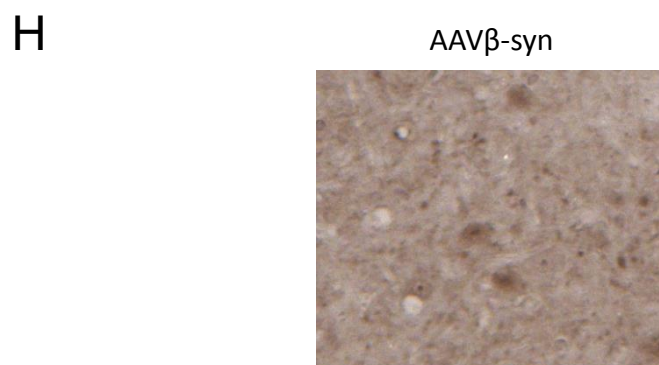
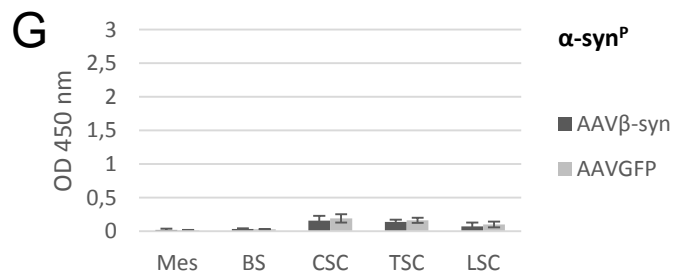
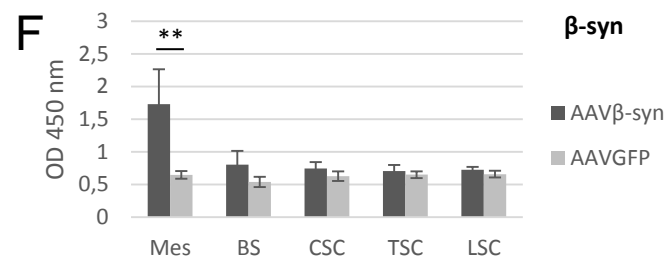
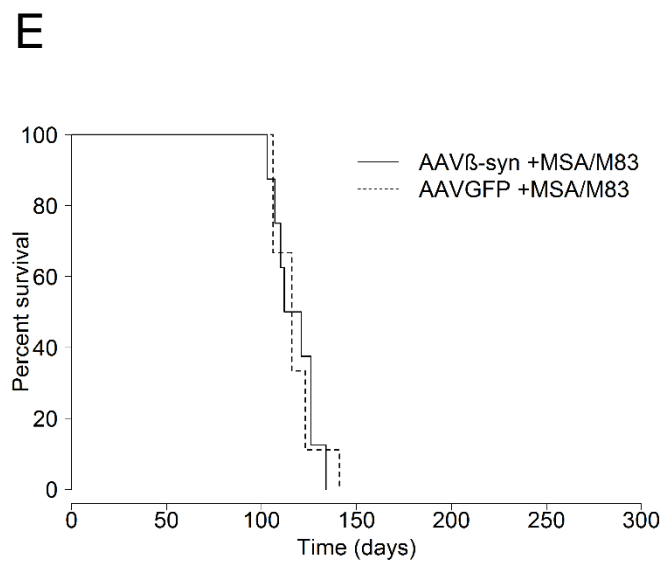
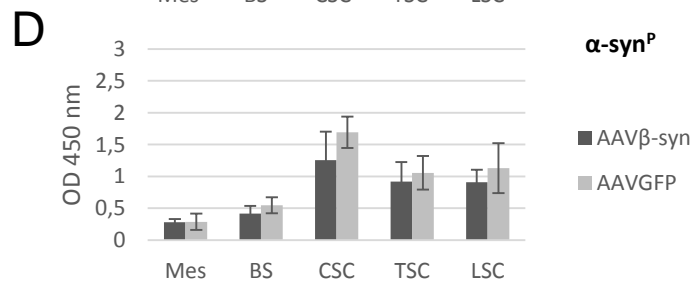
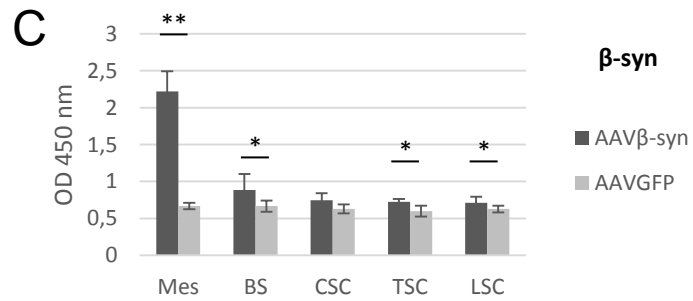
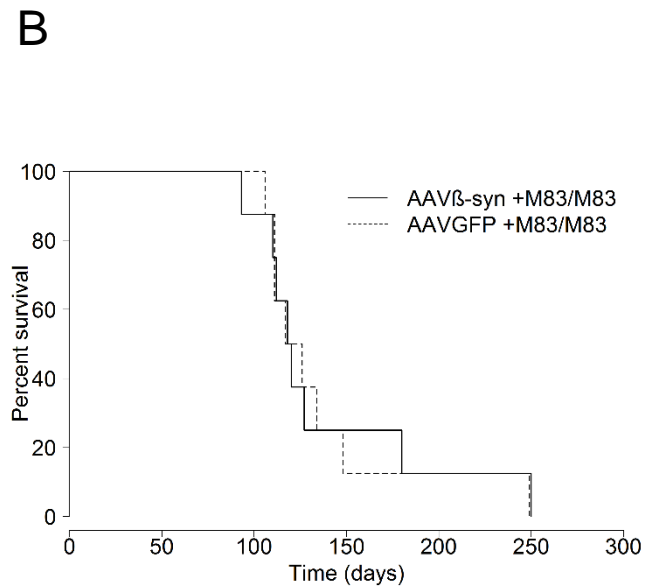
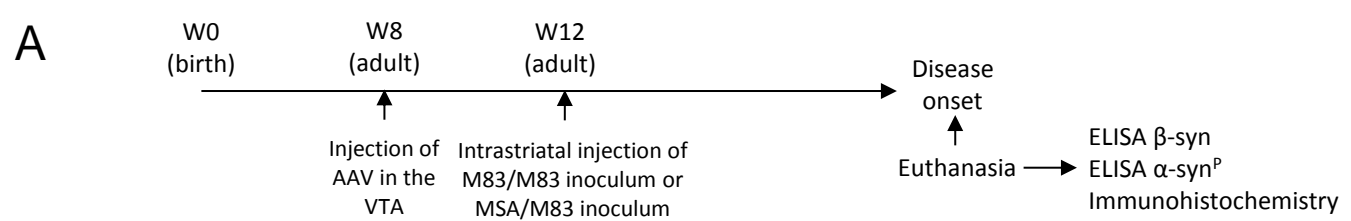
752

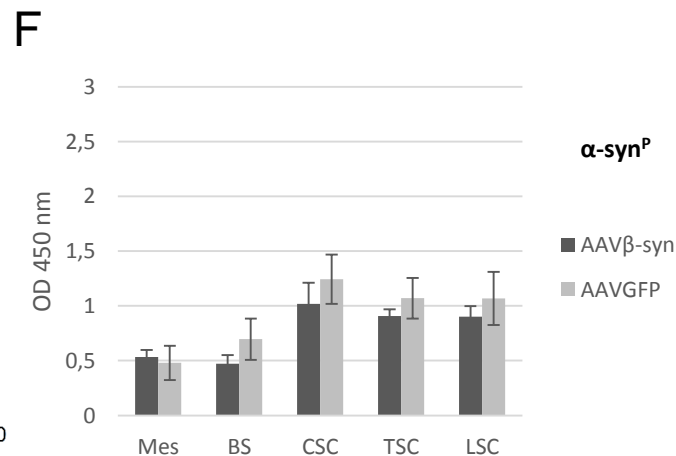
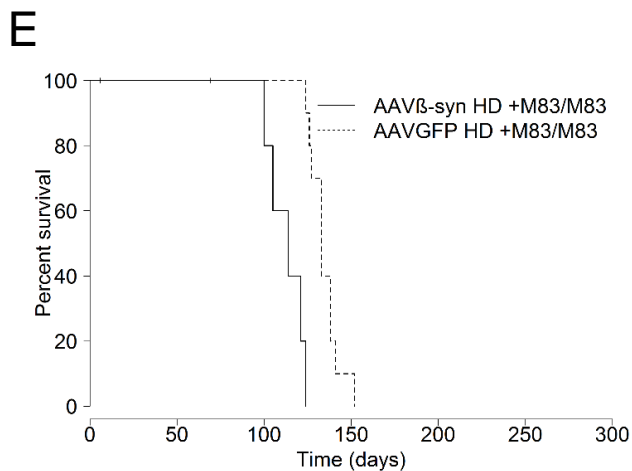
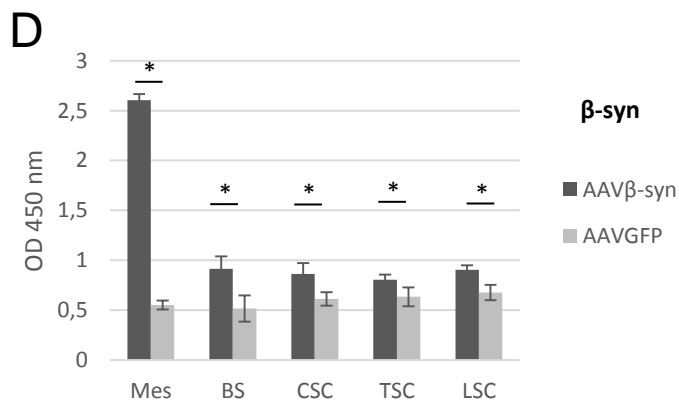
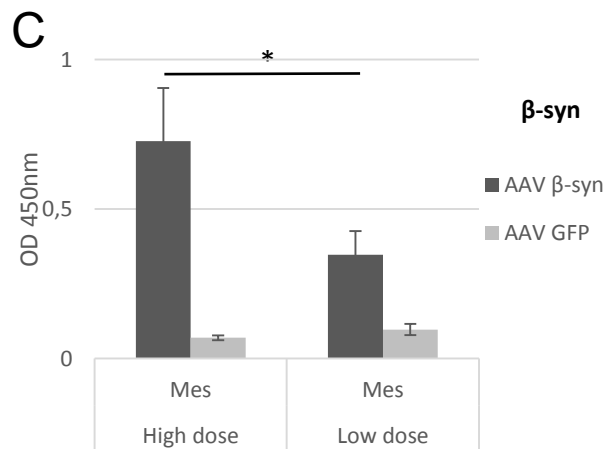
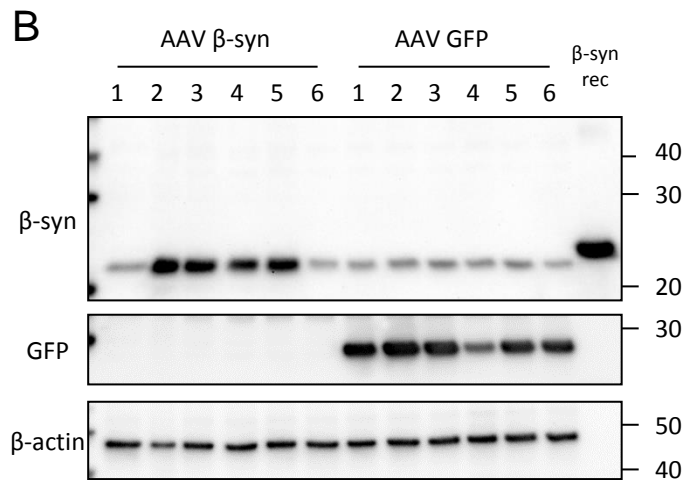
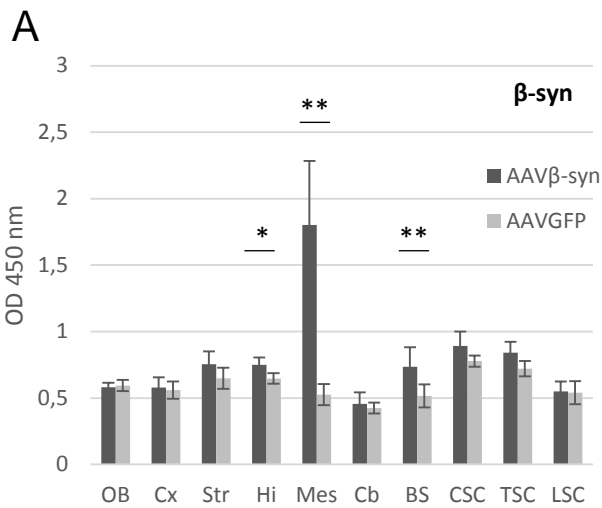
753 **Figure 6. Proteinase K (PK)-resistant  $\beta$ -syn staining in sick M83 mice inoculated with**  
754 **AAV  $\beta$ -syn.** (A-D) Immunoreactivity to total  $\beta$ -syn antibody in mesencephalon sections of  
755 two sick M83 mice inoculated with low dose of AAV $\beta$ -syn or AAVGFP in the VTA and  
756 challenged by MSA/M83 inoculum (mice from the study Figure 4E-G) is shown without PK  
757 digestion (A, B) or after PK digestion (C, D). After PK digestion, these  $\beta$ -syn immunoreactive  
758 dots were detected in all mice analyzed by immunohistochemistry inoculated with the AAV $\beta$ -  
759 syn in the VTA (7/7 mice, comprising 2 mice challenged with M83/M83 inoculum, 3 mice  
760 challenged with MSA/M83 inoculum, and also in 2 mice inoculated with high dose of AAV  
761 and challenged with M83/M83 inoculum), but not in sick M83 mice inoculated with  
762 AAVGFP (3/3, comprising 2 mice challenged with MSA/M83 inoculum and 1 mouse  
763 challenged with M83/M83 inoculum). Scale bars 100 $\mu$ m (low magnification) and 25 $\mu$ m (high  
764 magnification).



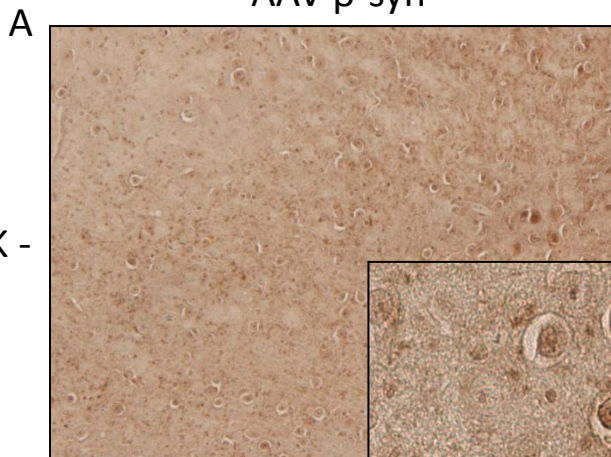
**A****B****C**







AAV  $\beta$ -syn



AAV GFP

